JOURNAL OF GUIDANCE, CONTROL, AND DYNAMICS
Vol. 23, No. 2, March–April 2000

Automatic Landing System Design Using Fuzzy Logic

Kyungmoon Nho* and Ramesh K. Agarwal†
Wichita State University, Wichita, Kansas 67260-0093

A fuzzy logic control system is developed for automatic landing control of both a linear and a nonlinear aircraft model. A linear longitudinal aircraft model, with landing gear and flaps deployed at the sea level, is employed for fuzzy logic controller design of automatic landing system including the two landing phases, the glide-path capture and the flare maneuver. In addition, the fuzzy control system is tested on a six-degree-of-freedom nonlinear aircraft model. It is shown that the simple tuning fuzzy controller, by altering scaling factors, is well suited for controlling the trajectory of the aircraft in the landing phase that requires simultaneous control of the engine thrust for changing the velocity and the elevator for changing the pitch attitude to change the altitude with a constant airspeed.

I. Introduction

In recent years, fuzzy-logic-based control law design has shown great promise in many industrial applications modeled by linear as well as nonlinear systems. In particular, there has been considerable progress in the application of adaptive fuzzy controllers to the control of complex nonlinear systems with uncertainty due to time-varying system parameters over a wide range of operating conditions.[1–3] The model-based adaptive fuzzy control techniques[4,5] have been successfully applied to many systems and have been shown to be globally stable. However, most of these techniques require modeling or parameter estimation of the plant, which is usually achieved by employing a complex identification procedure. Several other self-tuning techniques for the design of adaptive and optimal fuzzy controllers have been developed and successfully applied to the control of many industrial problems.

Although the conventional proportional-derivative (PD) and fuzzy logic controllers (FLCs) are not exactly comparable, the PD-type FLC is frequently used as a practical alternative to conventional methods for solving complex control problems.[6–9] It is well known that PD-type FLC, like the conventional PD controller, gives rapid response in the transient state, which results in reducing the time required to reach a desired set point or steady state. However, near the steady state, the values of FLC input variables, the error e and the change in error $\dot{e}$, are too small to deal with the steady-state error or other instabilities. In this paper, a simple tuning method based on switching of the scaling factors[10–14] of the fuzzy controller is proposed to get better performance for a variety of conditions. It is shown by simulation that the proposed scheme has the ability to improve the transient- and steady-state performance of the controlled system simultaneously. Scaling factors have the biggest impact in determining the system performance and stability. The input scaling factors of FLC transform a physical signal into the normalized universe of discourse of the controller. The output scaling factors provide the plant with crisp values by transforming the defuzzified output signal from the normalized universe of discourse of FLC output. The importance of suitable selection of input scaling factors is clearly shown by bad scaling resulting in unsatisfactory performance due to utilization of only a small area of the normalized universe of discourse. Furthermore, the selection of suitable output scaling factors affects the closed-loop gain, which has direct influence on system stability. In this paper, the output scaling factors are kept fixed for the sake of simplicity of FLC design.

A PD-type fuzzy control system is developed based on simple longitudinal medium-sized transport aircraft model for the glide-path capture and the flare landing phase. In addition, the fuzzy control system is modified for a nonlinear aircraft dynamics model in the glide path. Each resulting closed-loop system basically has the same fuzzy control parameters and structure except for different values of the scaling factors and FLC for lateral motion in the nonlinear aircraft model. An appropriate algorithm to select and switch the scaling factors of FLC is also proposed, based on the performance measure.

Received 19 August 1998; revision received 25 May 1999; accepted for publication 10 June 1999.

*Graduate Research Assistant. National Institute for Aviation Research. Student Member AIAA.

†Bloomfield Distinguished Professor and Executive Director. National Institute for Aviation Research. Fellow AIAA.

II. Problem Statement

The objective of this paper is to design a robust fuzzy control system for automatic control of the aircraft landing trajectory: both the glide-path capture and the flare maneuver. In this section, two aircraft models, a linear longitudinal model and a six-degree-of-freedom (DOF) nonlinear model, are described briefly. The plant employed for the design process is a linear longitudinal model that has fixed aerodynamic coefficients at a low-speed flight condition. Data are also included for the effects of landing gear and flaps. Typical Federal Aviation Administration landing specifications are employed for the desired flight paths for automatic landing.

A. Problem Description and Requirements

Automatic control of the landing trajectory of an aircraft is one of the most challenging tasks for an autopilot, requiring simultaneous control of several variables: velocity, flight-path angle, and altitude. The general problem is to design a robust fuzzy control system that satisfies the desired operational constraints over a wide range of flight conditions. Figure 1 shows a typical glide-path trajectory.

The performance of an automatic landing system depends highly on the accurate control of the glide-path capture, which is important both in terms of the stability of the aircraft and for providing a good starting point for the flare maneuver. The glide-path capture, which is characterized as a smooth transition from level flight to the desired flight-path angle (FPA) γ_d or trajectory, must be tightly controlled to achieve the safe flare maneuver. It is assumed that the automatic glide-path command for a nonlinear model simulation is initiated at about 1500-ft altitude with an airspeed of 260 ft/s and $\gamma_d = -2.6$ deg, which corresponds to a decent rate of 11.34 ft/s.

The glide-path deviation rate, that is, the velocity component perpendicular to the glide path, is defined by

$$\dot{d} = V_T \sin(\gamma - \gamma_d) \approx V_T(\gamma - \gamma_d) \tag{1}$$

In the glide-path tracking, it is required that d approaches zero so that the FPA γ becomes equal to γ_d. In addition, altitude h is also included as a state using the equation for the climb or descent rate

$$\dot{h} = V_T \sin\gamma \approx V_T(\theta - \alpha) \tag{2}$$

where α is the angle of attack and θ is the pitch attitude. The desired altitude is given by

$$\dot{h}_d = V_T \sin\gamma_d \tag{3}$$

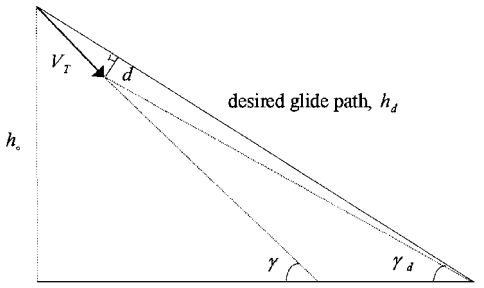

Fig. 1 Glide-path trajectory for automatic landing.

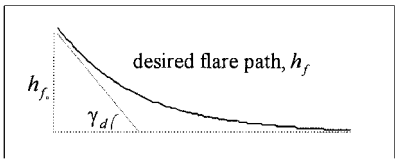

Fig. 2 Flare-path geometry.

Flare control is more difficult than the glide-path maneuver. At the start of flare, the rate of descent of the aircraft is reduced, and it must be decreased to less than about 2.0 ft/s before touchdown. The required pitch attitude at touchdown is between 0 and 5 deg, depending on the type of aircraft and the conditions at the start of the flare maneuver. The trajectory of the flare maneuver is shown in Fig. 2.

For the desired flare trajectory, an exponential flare command that decays exponentially from h_{f0} to zero is employed. The flare command model employed is given by

$$h_f = h_{f0}\, e^{-t/\tau} \Rightarrow \dot{h}_f = -(h_f/\tau) \tag{4}$$

with the initial vertical velocity of the flare equal to the rate of altitude of the glide path

$$h_f(0) = -\tau \dot{h}(0) = \tau V_T \sin\gamma_d \tag{5}$$

where $\tau = 2.667$ s and $h_{f0} = 30$ ft are used for simulation.

B. Aircraft Model Description

A simple longitudinal model for a medium-sized transport aircraft is employed in controller design for automatic landing using fuzzy logic for a nominal approach flight condition with landing gear and flaps deployed. The trim conditions are given by $V_T = 250$ ft/s, $\gamma = -2.5$ deg, $x_{cg} = 0.25\,\bar{c}$, and $H = 750$ ft (half-way down the glide slope). The aircraft weight is 162,000 lb. It has two turboprop engines, each developing 30,000 lb of static thrust at sea level. The wing area S is 2170 ft^2, the wing span is 140 ft, the average chord length $\bar{c}$ is 17.5 ft, the length is 90 ft, and the pitch-axis inertia is 4.1×10^6 slug-ft^2. The aircraft dynamics is described by

$$\dot{x} = Ax + Bu \tag{6}$$

where the states are

$$x = \begin{bmatrix} v_T \\ \alpha \\ \theta \\ q \\ h \end{bmatrix} = \begin{bmatrix} \text{longitudinal velocity} \\ \text{angle of attack} \\ \text{pitch attitude} \\ \text{pitch rate} \\ \text{altitude} \end{bmatrix} \tag{7}$$

and the control inputs are the engine thrust δ_{th} and the elevator deflection δ_e given in degrees as

$$u = [\delta_{th},\ \delta_e]^T \tag{8}$$

with the A and B Jacobian matrices for the given timed flight condition as

$$A = \begin{bmatrix} -0.038 & 18984 & -3214 & 0 & 1.32e{-}4 & 0 \\ -0.001 & -0.632 & 5.6e{-}3 & 1.0 & 3.75e{-}6 & 0 \\ 0 & 0 & 0 & 1.0 & 0 & 0 \\ 7.8e{-}5 & -0.759 & -7.9e{-}4 & -0.5183 & -3.08e{-}7 & 0 \\ -0.043 & -2497 & 249.76 & 0 & 0 & 0 \\ 0 & -2500 & 2500 & 0 & 0 & 0 \end{bmatrix} \tag{9}$$

and

$$B = \begin{bmatrix} 10.1 & 0 \\ -1.54e{-}4 & 0 \\ 0 & 0 \\ 2.46e{-}2 & -1.07e{-}2 \\ 0 & 0 \\ 0 & 0 \end{bmatrix} \tag{10}$$

The throttle servo and engine lag is modeled by 5-s lag and the elevator servo by 0.1-s lag, that is,

$$\dot{\delta}_{th} = -1/\tau_{th}\,\delta_{th} + 1/\tau_{th}\,\delta_{thcom} \tag{11}$$

and

$$\dot{\delta}_e = -1/\tau_e\,\delta_e + 1/\tau_e\,\delta_{ecom} \tag{12}$$

with $\tau_{th} = 5$ s and $\tau_e = 0.1$ s. The elevator servo is limited to deflection of ± 20.5 deg.

The primary goal of this paper is to design a fuzzy control system that is simple but robust enough to perform a difficult maneuver of a nonlinear aircraft model with the nonlinear coupling terms and other uncertain nonlinearities. The six-DOF nonlinear aircraft model employed in this paper is constructed from a scale model of an F-16 airplane tested in the NASA Langley Research Center wind tunnel. The data collected from the wind-tunnel test is reduced to obtain the approximate mathematical model. The aerodynamic forces and moments are calculated from the two-dimensional data lookup table and a linear interpolation routine. The wind-tunnel data includes a model of the F-16 afterburning turbofan engine. Complete descriptions of the longitudinal model of a medium-sized transport aircraft and the nonlinear model of an F-16 fighter aircraft are given in Ref. 15.

III. FLC

The successful design of a fuzzy control system for an automatic landing of an aircraft using the nonlinear aircraft dynamics is the key contribution of this paper. The fuzzy control system design starts with a simple longitudinal aircraft model given by Eqs. (9) and (10), rather than the nonlinear model that is employed at a later stage. The values of the FLC scaling factors selected for the longitudinal model are simply changed to obtain the fuzzy control system for the nonlinear aircraft dynamics. Note that the fuzzy control system developed for the longitudinal transport aircraft dynamics can be easily adapted to a nonlinear fighter aircraft model by changing the FLC scaling factors only. Note that the resulting fuzzy control system for the nonlinear aircraft dynamics contains two more FLCs for the lateral control inputs, that is, the aileron δ_a and the rudder δ_r.

In the conventional linear control theory, the transfer function of the proportional integral derivative (PID) controller is

$$K_P + (K_I/s) + K_D s \tag{13}$$

and the control signal based on the closed-loop error $e(t) = x_d - x(t)$ has the following standard form:

$$u(t) = K_P e(t) + K_I \int e(t)\,\mathrm{d}t + K_D \frac{\mathrm{d}e(t)}{\mathrm{d}t} \tag{14}$$

The variable $e(t)$ represents the tracking error, the difference between the desired value x_d and the actual output $x(t)$. K_P, K_I, and K_D are the proportional, the integral, and the derivative gains, respectively. PID-type FLC has a similar structure and parameter characteristics to the linear PID controller given by Eq. (13). The design of FLC based only on the PD controller is considered.

The design of FLC starts with the formulation of fuzzy control rules. The input of a PD-type FLC normally includes the error between the state variable and its set point, $e(=x_d - x)$, and the first derivative of the error, $\dot{e}$. These input variables are scaled as follows:

$$e = S_e e^* \tag{15}$$

and

$$\dot{e} = S_{\dot{e}} \dot{e}^* \tag{16}$$

where S_e and $S_{\dot{e}}$ are scaling factors for the input variables, the error and the error rate, respectively. A typical form of the linguistic rules is represented as

$$\text{Rule } i\text{th: IF } e \text{ is } A_i \text{ AND } \dot{e} \text{ is } B_i \text{ THEN } u^* \text{ is } C_i$$

where A_i, B_i, and C_i are the fuzzy sets for the error, the error rate, and the controller output at rule i, respectively, and u^* is the controller output. The resulting rule base of FLC is shown in Table 1. The abbreviations representing the fuzzy sets N, Z, P, S, and B in linguistic form stand for negative, zero, positive, small, and big, respectively, for example negative big (NB). Five fuzzy sets in triangular membership functions are used for FLC input variables, e and $\dot{e}$, and FLC output, u^*. The selection of rule base is explained by Fig. 3. For example, in the region of negative error $(e - N)$ and negative error rate $(\dot{e} - N)$, where the state is diverging, FLC is set up to produce a large control value to change the current state to the desired value or trajectory. Therefore, the output of FLC is set to PB.

For the fuzzy inference or rule firing, Mamdani-type min–max composition is employed. In the defuzzification stage, by adopting the method of center of gravity, the deterministic control u is obtained as follows:

$$\begin{aligned} u &= S_u \text{FLC}(S_e e, S_{\dot{e}} \dot{e}) \\ &= S_u u^* \\ &= S_u \frac{\sum_{j=1}^{k} u_j \mu_j(u_j)}{\sum_{j=1}^{k} \mu_j(u_j)} \end{aligned} \tag{17}$$

Table 1 Rule base for FLC

	Fuzzy set, $\dot{e}$				
Fuzzy set, e	NB	NS	Z	PS	PB
NB	PB	PB	PS	PS	NS
NS	PB	PB	PS	NS	NB
Z	PB	PS	Z	NS	NB
PS	PB	PS	NS	NS	NB
PB	PS	NS	NS	NB	NB

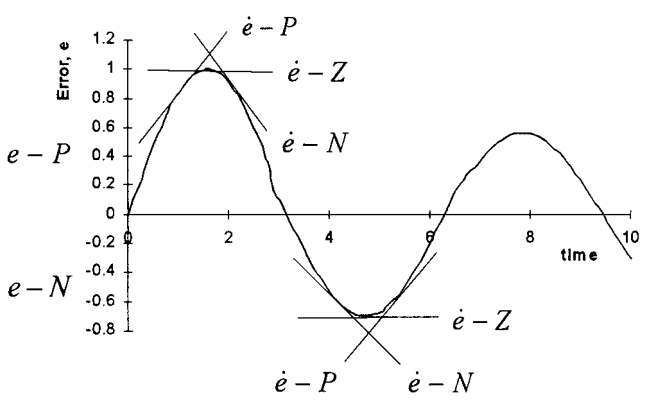

Fig. 3 Schematic explaining the fuzzy rule base of FLC.

Table 2 Effects of scaling factors

Scaling factor	Rise time	Overshoot	S-S error
S_e	Decrease	Increase	Decrease
$S_{\dot{e}}$	Increase	Decrease	Small change
S_u	Decrease	Increase	Decrease

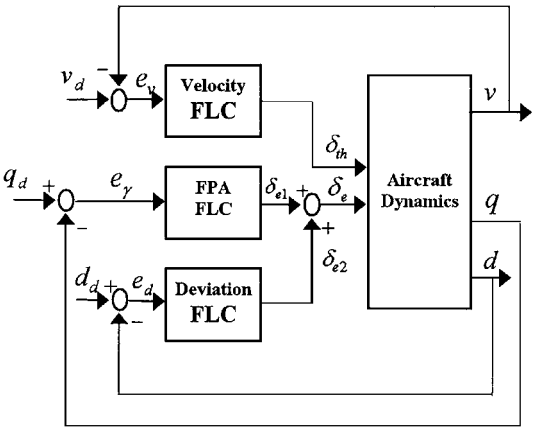

Fig. 4 Overall structure of fuzzy control system for the glide-path capture.

where S_u is the scaling factor for controller output, k is the number of quantization levels of the output, u_j is the control amount for a quantization level corresponding to an integer j closest to the real value, and $\mu_C(u_j)$ is its membership value in controller output fuzzy set C.

The values of scaling factors are selected considering three performance requirements: rise time, overshoot, and steady-state error. For example, when the controlled state position is far away from the desired value, the values of input scaling factors are selected based on reducing the rise time and then later switched to prevent overshoot as the system output approaches the required state. The output scaling factors are determined to limit the FLC output to a reasonable level. Another important role of the output scaling factors is to reduce the steady-state (S-S) error. Effects of each of the scaling factors S_e, $S_{\dot{e}}$, and S_u on a closed-loop system are summarized in Table 2. Note that these correlations may not be exactly accurate because S_e, $S_{\dot{e}}$, and S_u are dependent on each other and on the fuzzy rule base. The values of the scaling factors are intuitively determined; however they can be obtained more accurately using advanced optimization techniques such as genetic algorithms.

The overall structure of the control system for the glide-path command control is shown in Fig. 4. The key features of the three FLCs used in the glide-path capture are discussed next.

A. FLC for Pitch Stabilization

The FLC for pitch stability is employed to stabilize the pitch attitude at a particular value. The pitch attitude is changed until the required constraint, for example, zero deviation error, or a desired FPA is met. Another important role of this FLC is to provide a satisfactory control of both the natural frequency and the damping of the longitudinal dynamics. The pitch-axis stability is achieved by employing the pitch rate as the feedback signal. The block diagram of FLC for pitch attitude stabilization is shown in Fig. 5. To stabilize the pitch attitude efficiently during the glide-path maneuver, scaling factors for fuzzy input variables are switched between two predefined values. For example, when the error e, used as the performance measure, reaches a given threshold value TH_e, the initial input error scaling factor $S1_e$ is switched to a larger value $S2_e$, to produce large enough control output to reduce the S-S error by raising the sensitivity of the FLC. Note that the value of the initial input error scaling factor $S1_e$ is selected based on reducing the rise time. On the other hand, the input error rate scaling factor $S1_{\dot{e}}$ is initialized to a large value and then switched to a smaller value $S2_{\dot{e}}$, which results in increasing the damping and reducing the overshoot. In this work, the controller output scaling factor $S_{\delta_{e1}}$ is fixed and determined

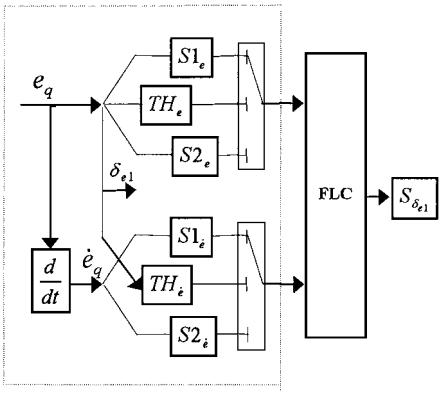

Fig. 5 Schematic of scaling factor switch in FLC for FPA.

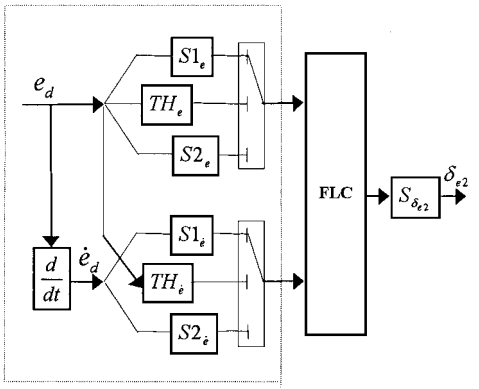

Fig. 6 Schematic of scaling factor switch in FLC for deviation error.

considering the overall stability and performance of the system and to limit the controller output.

B. FLC for Deviation Error

The main goal of automatic controller design for the glide-path capture is to command an aircraft to follow a given trajectory. The block diagram of FLC for controlling the deviation error is shown in Fig. 6. This is identical to the FLC used for pitch stabilization control, except for the different values of the scaling factors employed for fuzzy controller input and output variables. The glide-path or altitude deviation error and its error rate obtained from Eq. (1) are used as FLC input variables. The FLC for deviation error is aimed at driving the deviation error back to zero, which consequently results in keeping the FPA to a desired value. To achieve this goal successfully, the FLC output δ_{e2} is simply added to the output of FLC for pitch attitude stabilization, and thus, the resulting elevator deflection angle becomes $\delta_e = \delta_{e1} + \delta_{e2}$. Note that the value of the deviation FLC output scaling factor depends on that of pitch FLC. In fact, changing $S_{\delta_{e2}}$ can change the effect of $S_{\delta_{e1}}$. The value of $S_{\delta_{e2}}$ is selected to be less than that of $S_{\delta_{e1}}$ which is intended to put more emphasis on aircraft longitudinal stability.

C. FLC for Velocity

In addition to the pitch attitude stabilization and altitude control by the elevator, a complete automatic landing is accomplished by designing the engine thrust controller to keep the aircraft speed constant. The aircraft speed control in the landing approach is critical to hold the required trajectory by providing the aircraft with the necessary aerodynamic forces. The same structure as shown for the previous two FLCs in Figs. 5 and 6 is employed for the FLC for engine thrust control, except again for different values of the scaling factors.

IV. Numerical Simulations

A. Simulations Using a Linear Longitudinal Transport Aircraft Model

The initial conditions employed in simulation of an automatic landing for the glide-path capture using a linear longitudinal transport aircraft model are as follows: $v_T(0) = 20$ ft/s, $\alpha(0) = -0.1$ rad, $\theta(0) = 0.1$ rad, $q(0) = 0$ rad/s, $d(0) = 0$ ft, and $h(0) = 1500$ ft. The initial conditions employed for the flare maneuver are as follows: $v_T(0) = 0$ ft/s, $\alpha(0) = 0$ rad, $\theta(0) = -0.04$ rad, $q(0) = 0$ rad/s, $h_d(0) = 30$ ft, and $h(0) = 30$ ft.

The simulation results employing a linear longitudinal transport aircraft model for an automatic landing, including the glide-path capture and the flare control, are shown in Figs. 7–16. Figures 7 and 8, respectively, show that the actual and desired glide-path trajectories converge quickly, and the deviation error becomes negligible. Figure 9 shows that the FPA is held near the desired constant value, $\gamma_d = -0.045$ rad. Figure 10 shows that the disturbed initial airspeed is reduced to a desired value $v_T = 0$ ft/s smoothly without overshoot. The time response of throttle for engine thrust and elevator deflection during the glide-path maneuver are shown in Figs. 11 and 12, respectively.

For the final portion of the landing approach, the flare maneuver simulation results are shown in Figs. 13–16. Figure 13 shows that the difference between the actual and desired trajectories is kept less than about 6 ft. Figure 14 shows that the pitch attitude at touchdown remains within ±1% of the desired value. Figure 15 shows that the sink rate (the rate of descent) is reduced to less than 2.0 ft/s, which is small enough to achieve a smooth landing. The throttle for engine thrust and elevator deflection during flare are shown in Fig. 16.

B. Simulations Using a Nonlinear Fighter Aircraft Model

To ascertain the handling capability of fuzzy logic controller, a six-DOF nonlinear fighter aircraft model is employed, and the simulations are performed for the glide-path capture using the FLCs developed for the linear longitudinal transport aircraft model.

The initial conditions, based on trim data, employed in simulation of an automatic landing for the glide-path capture using a nonlinear F-16 fighter aircraft model are as follows: V_T

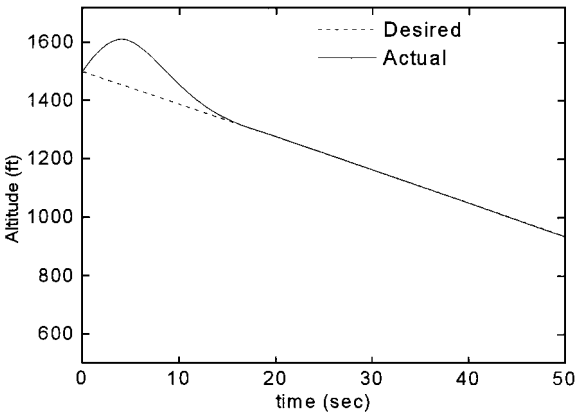

Fig. 7 Desired and actual glide-path trajectories.

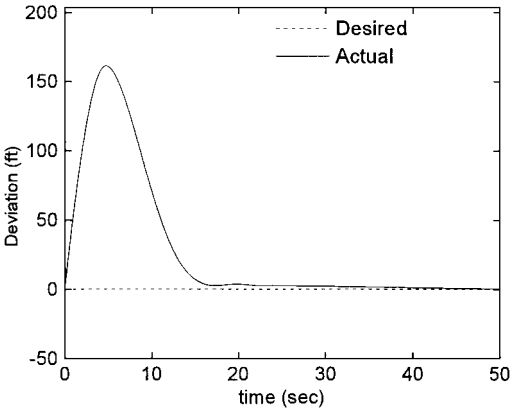

Fig. 8 Time response of the glide-path deviation.

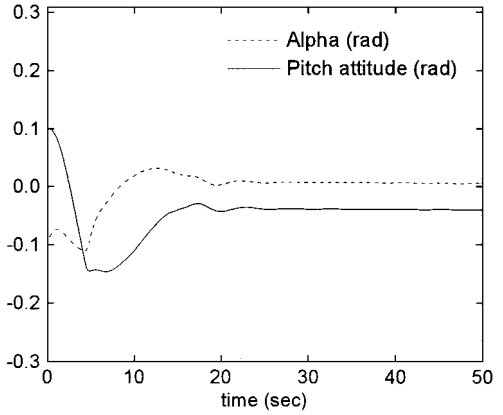

Fig. 9 Time response of the angle of attack and the pitch attitude during glide path.

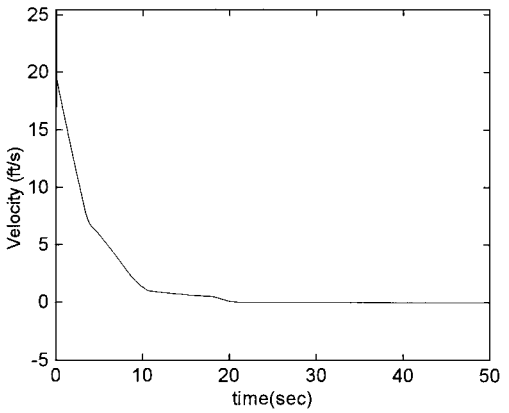

Fig. 10 Time response of velocity during glide path.

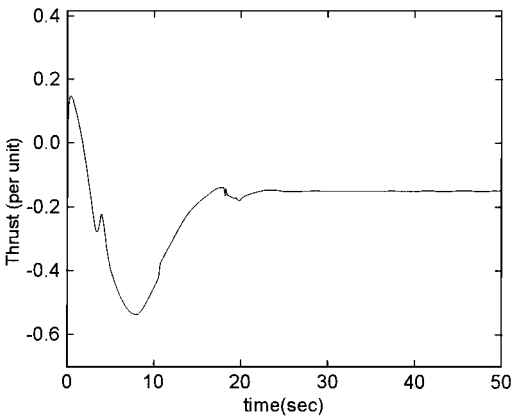

Fig. 11 Time response of engine throttle during glide path.

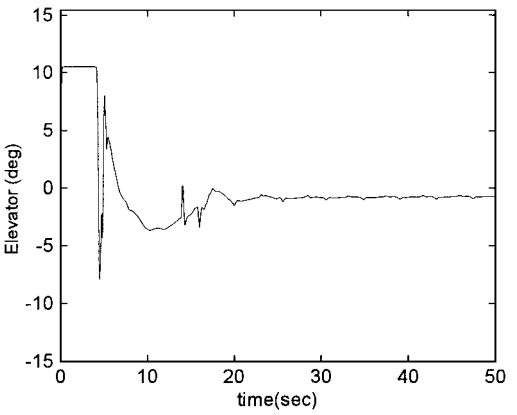

Fig. 12 Time response of elevator during glide path.

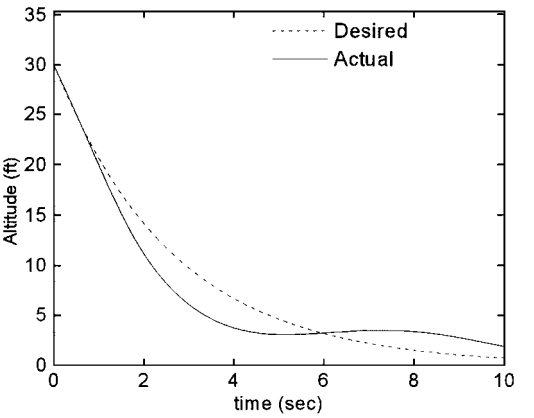

Fig. 13 Desired and actual flare trajectories.

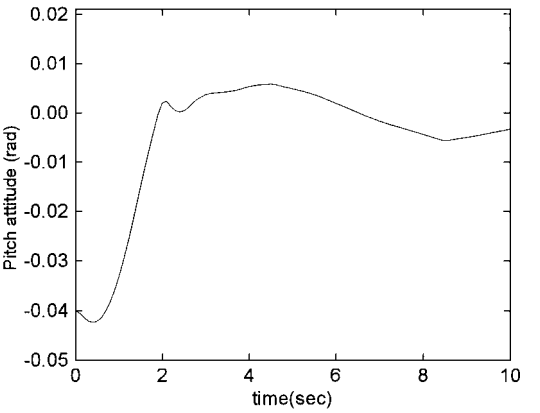

Fig. 14 Time response of the pitch attitude in flare.

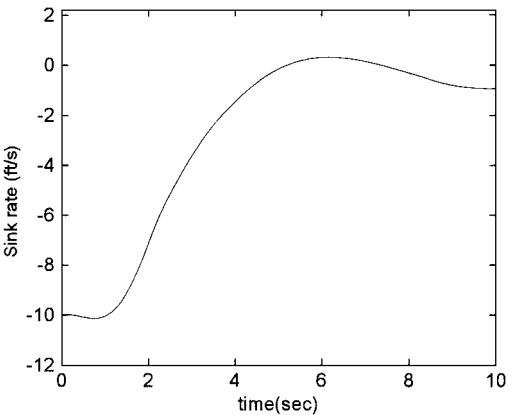

Fig. 15 Sink rate during the desired flare trajectory.

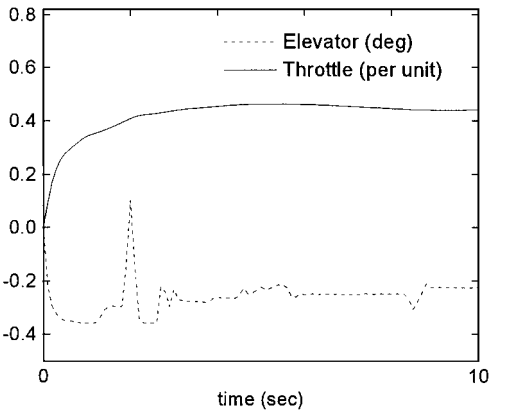

Fig. 16 Time response of elevator and engine throttle during flare.

(true airspeed) = 260 ft/s, α (angle of attack) = 2.12e−4 rad, β (side-slip angle) = −3.6e−9 rad, Φ (roll angle) = 0.1 rad, Θ (pitch angle) = 2.151e−1 rad, Ψ (yaw angle) = −0.1 rad, P (roll rate) = 0 rad/s, Q (pitch rate) = 0 rad/s, R (yaw rate) = 0 rad/s, and H (altitude) = 1500 ft.

The command inputs for this case are V_{T_d} = 250 ft/s and γ_d = −0.045 rad. Note that the structure of the fuzzy control system employed for the nonlinear aircraft model is basically the same as for the preceding simple longitudinal aircraft model except for different values of the input and output scaling factors and two additional FLCs needed for lateral control inputs. As shown in Fig. 17, in spite of the unstable longitudinal dynamics and nonlinearities of the aircraft model, the successful glide-path maneuver is achieved by keeping the actual glide path close to the desired trajectory. The time response of the deviation is shown in Fig. 18. It is

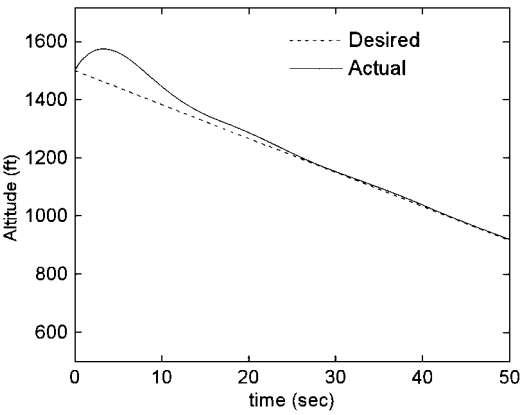

Fig. 17 Time response of the desired and actual glide-path trajectories.

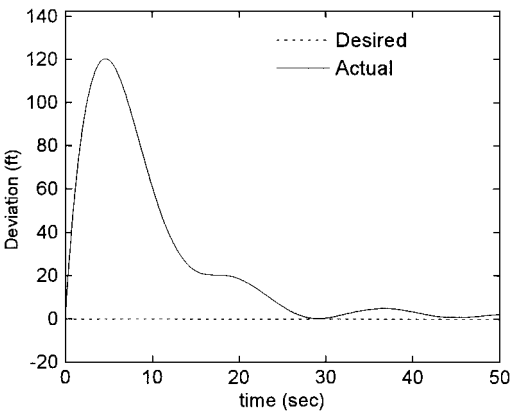

Fig. 18 Time response of the glide-path deviation.

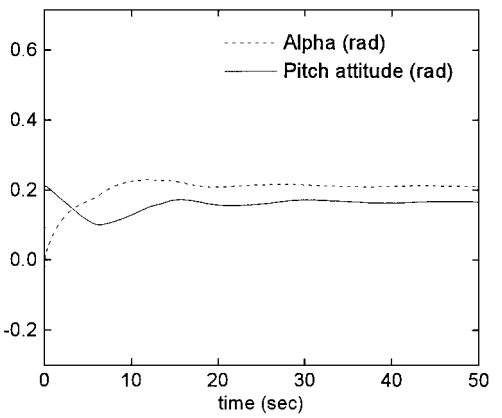

Fig. 19 Time response of the angle of attack and pitch attitude.

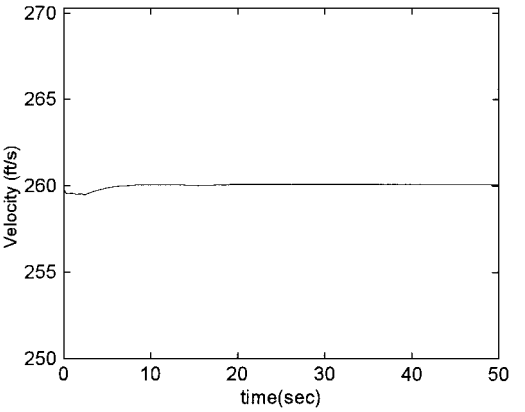

Fig. 20 Time response of the airspeed.

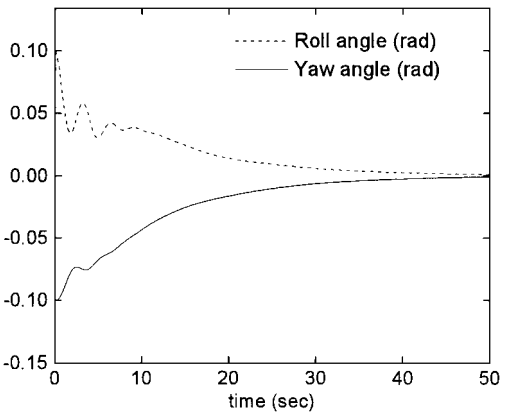

Fig. 21 Time response of bank and yaw angles.

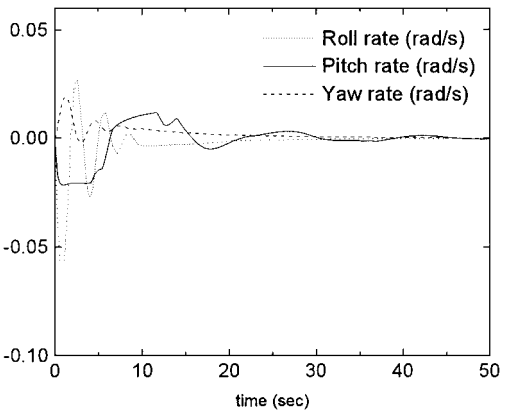

Fig. 22 Time response of roll, pitch, and yaw rate.

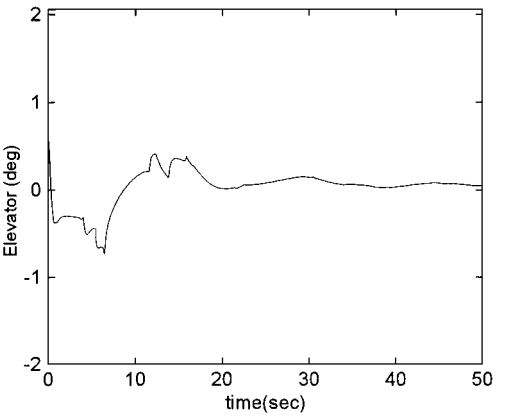

Fig. 23 Time response of elevator.

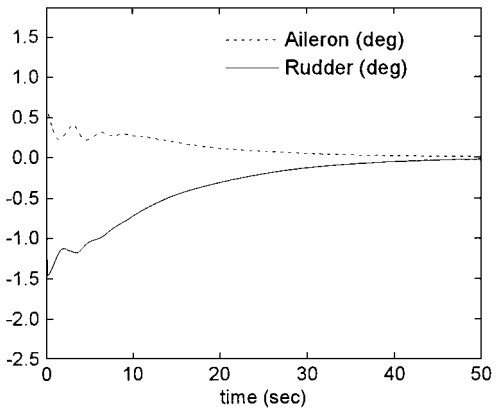

Fig. 24 Time response of aileron and rudder.

observed in Figs. 19 and 20, respectively, that the FPA and airspeed are held near the desired constant values as well. The time response of bank and yaw angles and roll, pitch, and yaw rates are shown in Figs. 21 and 22, respectively. The elevator control input is shown in Fig. 23. The resulting lateral control inputs during glide-path capture are shown in Fig. 24.

V. Conclusions

The goal of this work has been to demonstrate the successful application of FLC to the design of an automatic landing system. The primary advantages of a fuzzy controller are its simple design, its robustness for a wide range of initial conditions, and its ability to account for nonlinearity. The simulations for an automatic landing system are performed using both a linear longitudinal aircraft model and a nonlinear aircraft-dynamics model. It is shown that a simple tuned fuzzy control system designed for a longitudinal aircraft model is robust enough to give satisfactory performance, both in terms of stability and negligible S-S error, for a nonlinear aircraft-dynamics model as well.

References

[1]Wang, L. X., "Stable Adaptive Fuzzy Control of Nonlinear Systems," *IEEE Transactions on Fuzzy Systems*, Vol. 1, No. 2, 1993, pp. 146–155.

[2]Sasiadek, J. Z., and Mazzawi, A. N., "Fuzzy and Adaptive Control of an Aircraft," *Proceedings of the AIAA Guidance, Navigation, and Control Conference*, AIAA, Washington, DC, 1994, pp. 391–400.

[3]Wang, H. O., Tanaka, K., and Griffin, M. F., "An Approach to Fuzzy Control of Nonlinear Systems: Stability and Design Issues," *IEEE Transactions on Fuzzy Systems*, Vol. 4, No. 1, 1996, pp. 14–23.

[4]Takagi, T., and Sugeno, M., "Fuzzy Identification of Systems and Its Applications to Modeling and Control," *IEEE Transactions on Systems, Man, and Cybernetics*, Vol. 15, No. 1, 1985, pp. 116–132.

[5]Kung, Y. S., and Liaw, C. M., "A Fuzzy Controller Improving a Linear Model Following Controller for Motor Drives," *IEEE Transactions on Fuzzy Systems*, Vol. 2, No. 3, 1994, pp. 194–202.

[6]Wang, L. X., "Stable Adaptive Fuzzy Controllers with Application to Inverted Pendulum Tracking," *IEEE Transactions on Systems, Man, and Cybernetics*, Vol. 26, No. 5, 1996, pp. 677–691.

[7]Oh, S. K., Park, J. J., and Woo, K. B., "The Optimal Tuning Algorithm for Fuzzy Controller," *Proceedings of the Fifth IFSA World Congress*, International Fuzzy Systems Associates, 1993, pp. 830–833.

[8]Driankov, D., Hellendoorn, H., and Reinfrank, M., *An Introduction to Fuzzy Control*, Springer–Verlag, New York, 1993, pp. 197–244.

[9]Viljamaa, P., and Koivo, H. N., "Tuning of a Multivariable Fuzzy Logic Controller," *Intelligent Automation and Soft Computing*, Vol. 1, No. 1, 1995, pp. 15–28.

[10]Malki, H. A., Li, H., and Chen, G., "New Design and Stability Analysis of Fuzzy Proportional-Derivative Control Systems," *IEEE Transactions on Fuzzy Systems*, Vol. 2, No. 4, 1994, pp. 245–254.

[11]Wong, C. C., and Feng, S. M., "A Switching Type of Fuzzy Controller," *Proceedings of the IEEE Conference on Decision and Control*, Inst. of Electrical and Electronics Engineers, New York, 1994, pp. 30–34.

[12]Qin, S. J., and Borders, G., "A Multiregion Fuzzy Logic Controller for Nonlinear Process Control," *IEEE Transactions on Fuzzy Systems*, Vol. 2, No. 1, 1994, pp. 74–81.

[13]Hayashi, S., "Auto-Tuning Fuzzy PI Controller," *Proceedings of the IFSA '91*, International Fuzzy Systems Associates, 1991, pp. 41–44.

[14]Nho, K., and Agarwal, R. K., "Application of Fuzzy Logic to Wing Rock Motion Control," AIAA Paper 98-0497, 36th Aerospace Sciences Meeting, Reno, NV, Jan. 1998.

[15]Stevens, B. L., and Lewis, F. L., *Aircraft Control and Simulation*, Wiley, New York, 1992.